Int J Thermophys (2009) 30:669–692
DOI 10.1007/s10765-008-0552-4

Thermo-mechanical Deformation in Magneto-micropolar Elastic Medium

Rajneesh Kumar · Rupender

Received: 4 September 2006 / Accepted: 3 December 2008 / Published online: 8 January 2009

Abstract The present investigation is concerned with a two-dimensional problem in electromagnetic micropolar elasticity for a half-space whose surface is subjected to distributed (concentrated or continuous) thermo-mechanical sources in the presence of a transverse magnetic field. As an application of the approach, the sources are taken as uniformly or linearly distributed. Laplace and Fourier transform techniques are used to solve the problem. The integral transforms have been inverted by using a numerical technique to obtain the components of normal strain, normal stress, tangential couple stress, and temperature distribution in the physical domain. Magnetic effects on the components of normal strain, normal stress, tangential couple stress, and temperature distribution have been depicted graphically for two different theories of generalized thermoelasticity, Lord and Shulman (L–S) theory and Green and Lindsay (G–L) theory. A particular case of interest is also deduced from the present investigation.

Keywords Magneto-micropolar thermoelasticity · Integral transforms · Thermo-mechanical sources

1 Introduction

The theory of magneto-elasticity was developed with the possibility of extensive practical applications in diverse fields such as geophysics, optics, acoustics, plasma

R. Kumar (✉) · Rupender
Department of Mathematics, Kurukshetra University,
Kurukshetra 136119, Haryana, India
e-mail: rajneesh_kuk@rediffmail.com

Rupender
e-mail: rupee_kuk@rediffmail.com

physics, etc. Surveys of relevant magneto-elasticity theories were presented by Knopoff [1], Banos [2], Chadwick [3], Purushothama [4], and Willson [5]. It is assumed that the electro-magnetic field influences the electric field by entering the elastic stress equation of motion as a body force called the Lorentz force. Then, the elastic field, in turn, influences the electromagnetic fields through modifications of Ohm's law. Consequently, such problems have been the subject of active research over the last few decades.

Modern engineering structures are often made of materials possessing an internal structure. Polycrystalline materials and materials with fibrous or coarse grain structure fall in this category. Classical elasticity is inadequate to represent the behavior of such materials. The analysis of such materials requires incorporation of the theory of oriented media. "Micropolar elasticity," as termed by Eringen [6], is used to describe deformation of elastic media with oriented particles. A micropolar continuum is a collection of interconnected particles in the form of small rigid bodies undergoing both translational and rotational motions. Typical examples of such materials are granular media and multi-molecular bodies, whose microstructures act as an evident part in their macroscopic responses. The physical nature of these materials needs an asymmetric description of deformation, while theories for classical continua fail to accurately predict their physical and mechanical behavior. For this reason, micropolar theories were developed by Eringen [6–8] for elastic solids, fluids, and also for nonlocal polar fields and are now universally accepted.

The classic theory of thermoelasticity is based on Fourier's law which predicts an infinite speed of heat propagation. In order to eliminate this paradox of an infinite speed of thermal propagation, two generalizations to the coupled theory have been considered.

The first is due to Lord and Shulman [9], who introduced the theory of generalized thermoelasticity with one relaxation time. This theory is based on a new law of heat conduction to replace Fourier's law. The heat equation is replaced by a hyperbolic one which ensures finite speeds of propagation for heat and elastic waves.

The theory of generalized thermoelasticity with two relaxation times was first introduced by Muller [10]. A more explicit version was then introduced by Green and Laws [11], Green and Lindsay [12], and independently by Suhubi [13]. In this theory the temperature rates are considered among the constitutive variables. This theory also predicts finite speeds of propagation as in Lord and Shulman's theory. It differs from the latter in that Fourier's law of heat conduction is not violated if the body under consideration has a center of symmetry.

Kalaski [14] derived the basic equation of thermo-magneto-micropolar elasticity. Kalaski and Nowacki [15] investigated the wave type of equations of thermo-magneto-micropolar elasticity. Nowacki [16] studied some problems of micropolar magneto-elasticity. Charderasekhariah [17,18] investigated magneto-thermal-elastic plane waves in micropolar elasticity. Ezzat and Youssef [19] investigated the problem of magneto-thermo-elasticity in a perfectly conducting media. Baksi et al. [20] studied magneto-thermo-elastic problems with thermal relaxation and heat sources in three-dimensional infinite rotating elastic media. In spite of these studies, little work has been carried out on the theory of magneto-micropolar thermoelasticity.

The aim of the present study is to investigate the interaction in magneto-micropolar thermoelastic material due to uniformly or linearly (concentrated/continuous) distributed thermo-mechanical sources.

2 Basic Equations

The simplified linear equations of electrodynamics of a slowly moving medium for a homogeneous and perfectly conducting elastic solid are the following:

$$\nabla \times \vec{h} = \vec{J} + \varepsilon_0 \frac{\partial \vec{E}}{\partial t}, \tag{1}$$

$$\nabla \times \vec{E} = -\mu_0 \frac{\partial \vec{h}}{\partial t}, \tag{2}$$

$$\vec{E} = -\mu_0 \left(\frac{\partial \vec{u}}{\partial t} \times \vec{H}_0 \right), \tag{3}$$

$$\nabla \cdot \vec{h} = 0. \tag{4}$$

Maxwell stress components are given by

$$T_{ij} = \mu_0 \left(H_i h_j + H_j h_i - H_k h_k \delta_{ij} \right), \tag{5}$$

where $\vec{H}_0$ is the external applied magnetic field intensity vector, $\vec{h}$ is the induced magnetic field vector, $\vec{E}$ is the induced electric field vector, $\vec{J}$ is the current density vector, $\vec{u}$ is the displacement vector, μ_0 and ε_0 are the magnetic and electric permeabilities, respectively, T_{ij}'s are the components of Maxwell stress tensor, and δ_{ij} is the Kronecker delta.

Equations 1–4 are supplemented by the field of equations of motion and constitutive relations in the theory of micropolar thermoelasticity, taking into account the Lorentz force;

$$\begin{aligned} &(\lambda + 2\mu + K) \nabla (\nabla \cdot \vec{u}) - (\mu + K) \nabla \times (\nabla \times \vec{u}) + K \left(\nabla \times \vec{\phi} \right) \\ &+ \vec{F} - \nu \left(1 + \tau_1 \frac{\partial}{\partial t} \right) \nabla T = \rho \frac{\partial^2 \vec{u}}{\partial t^2}, \end{aligned} \tag{6}$$

$$(\alpha + \beta + \gamma) \nabla \left(\nabla \cdot \vec{\phi} \right) - \gamma \nabla \times \left(\nabla \times \vec{\phi} \right) + K (\nabla \times \vec{u}) - 2K \vec{\phi} = \rho j \frac{\partial^2 \vec{\phi}}{\partial t^2}, \tag{7}$$

$$K^*\nabla^2 T = \rho c^* \left(\frac{\partial}{\partial t} + \tau_0 \frac{\partial^2}{\partial t^2}\right) T + \nu T_0 \left(\frac{\partial}{\partial t} + \tau_0 n_0 \frac{\partial^2}{\partial t^2}\right) (\nabla \cdot \vec{u}), \tag{8}$$

$$\sigma_{ij} = \lambda u_{r,r}\delta_{ij} + \mu \left(u_{i,j} + u_{j,i}\right) + K \left(u_{j,i} - \varepsilon_{ijr}\phi_r\right) - \nu \left(1 + \tau_1 \frac{\partial}{\partial t}\right) T\delta_{ij}, \tag{9}$$

$$m_{ij} = \alpha\phi_{r,r}\delta_{ij} + \beta\phi_{i,j} + \gamma\phi_{j,i}, \tag{10}$$

where $\lambda, \mu, K, \alpha, \beta, \gamma$ are the material constants, T is the temperature change, T_0 is the uniform temperature, K^* is the thermal conductivity, c^* is the specific heat at constant temperature, $\nu = (3\lambda + 2\mu + K)\,\alpha_t$, α_t is the linear thermal expansion, τ_0 and τ_1 are thermal relaxation times, ρ is the density, j is the microinertia, $\vec{\phi}$ is the microrotation vector, ∇ is the gradient operator, σ_{ij} are the components of the force tensor, m_{ij} are the components of couple stress tensor, ε_{ijk} is the alternate tensor, and $\vec{F}$ is the Lorentz force given by

$$\vec{F} = \mu_0 \left(\vec{J} \times \vec{H}_0\right). \tag{11}$$

For the L–S theory, $\tau_1 = 0,\ n_0 = 1$; for the G–L theory, $\tau_1 > 0, n_0 = 0$. The thermal relaxation times, τ_0 and τ_1, satisfy the inequality $\tau_1 \geqslant \tau_0 > 0$ for G–L theory only.

In vacuum, contacting the micropolar elastic half space, the system of equations of electrodynamics is

$$\nabla \times \vec{h}^0 = \varepsilon_0 \frac{\partial \vec{E}^0}{\partial t}, \tag{12}$$

$$\nabla \times \vec{E}^0 = -\mu_0 \frac{\partial \vec{h}^0}{\partial t}, \tag{13}$$

$$\nabla \cdot \vec{h}^0 = 0, \tag{14}$$

where $\vec{h}^0$ and $\vec{E}^0$ are the induced magnetic and electric field vectors, respectively, in vacuum. The above equations reduce to

$$\left(\nabla^2 - \frac{1}{c^2}\frac{\partial^2}{\partial t^2}\right) \vec{h}^0 = 0, \tag{15}$$

where c is the velocity of light given by

$$c = \frac{1}{\sqrt{\mu_0 \varepsilon_0}},$$

and ∇^2 is the Laplacian operator.

In this case, the Maxwell stress becomes

$$T_{ij}^0 = \mu_0 \left(H_i h_j^0 + H_j h_i^0 - H_k h_k^0 \delta_{ij} \right), \tag{16}$$

and T_{ij}^0 are the components of the Maxwell stress tensor in vacuum.

3 Formulation and Solution of the Problem

We consider a homogeneous, isotropic, perfectly conducting micropolar thermoelastic half-space ($y \geq 0$), in contact with vacuum, permeated by an initial magnetic field $\vec{H}^0$ acting along the z-axis, in both the media. The rectangular Cartesian co-ordinate system (x, y, z) having an origin on the surface $y = 0$, where the y-axis points vertically into the medium is introduced.

For the two-dimensional problem, we assume the displacement vector $\vec{u}$ and microrotation vector $\vec{\phi}$ as

$$\vec{u} = (u, v, 0) \quad \text{and} \quad \vec{\phi} = (0, 0, \phi_3) \tag{17}$$

We define the dimensionless quantities as

$$\begin{aligned} x' &= \frac{\bar{\omega}}{c_1} x, \quad y' = \frac{\bar{\omega}}{c_1} y, \quad u' = \frac{\rho c_1 \bar{\omega}}{\nu T_0} u, \quad v' = \frac{\rho c_1 \bar{\omega}}{\nu T_0} v, \quad \sigma'_{ij} = \frac{\sigma_{ij}}{\nu T_0} \\ T'_{ij} &= \frac{T_{ij}}{\nu T_0}, \quad m'_{ij} = \frac{\bar{\omega}}{c_1 \nu T_0} m_{ij}, \quad t' = \bar{\omega} t, \quad \tau'_1 = \bar{\omega} \tau_1, \quad \tau'_0 = \bar{\omega} \tau_0, \\ \phi'_3 &= \frac{\rho c_1^2}{\nu T_0} \phi_3, \quad h' = \frac{h}{H_0}, \quad T' = \frac{T}{T_0}, \end{aligned} \tag{18}$$

where

$$\bar{\omega} = \frac{\rho c^* c_1^2}{K^*}, \quad c_1^2 = \frac{\lambda + 2\mu + K}{\rho}.$$

Using the expressions relating the displacement components $u(x, y, t)$ and $v(x, y, t)$ to the scalar potential functions $\psi_1(x, y, t)$ and $\psi_2(x, y, t)$ in dimensionless form,

$$u = \frac{\partial \psi_1}{\partial x} + \frac{\partial \psi_2}{\partial y}, \quad v = \frac{\partial \psi_1}{\partial y} - \frac{\partial \psi_2}{\partial x}. \tag{19}$$

and applying the Laplace and Fourier transforms defined by

$$\bar{f}(x, y, s) = \int_0^\infty \mathrm{e}^{-st} f(x, y, t) \mathrm{d}t,$$

and

$$\tilde{f}(\xi, y, s) = \int_{-\infty}^{\infty} e^{i\xi x} \bar{f}(x, y, s)\, dx, \tag{20}$$

on Eqs. 6–8 and 15 and with the help of Eqs. 1, 3, 11, 17, and 18, we obtain

$$\left(\frac{d^4}{dy^4} + A\frac{d^2}{dy^2} + B\right)\tilde{\psi}_1 = 0, \tag{21}$$

$$\left(\frac{d^4}{dy^4} + C\frac{d^2}{dy^2} + D\right)\tilde{\psi}_2 = 0, \tag{22}$$

$$\left(\frac{d^2}{dy^2} - \lambda_5^2\right)\tilde{h}_0 = 0, \tag{23}$$

where

$$A = -2\xi^2 - \frac{s}{(1+a_1)}\{1+a_1+a_3\varepsilon\} - \frac{s^2}{(1+a_1)}\{a_4+(1+a_1)\tau_0+a_3\varepsilon(\tau_1+n_0\tau_0)\},$$

$$B = \xi^4 + \frac{s\xi^2}{(1+a_1)}\{1+a_1+a_3\varepsilon\} + \frac{s^2\xi^2}{(1+a_1)}\{a_4+(1+a_1)\tau_0+a_3\varepsilon(\tau_1+n_0\tau_0)\} + \frac{a_4}{(1+a_1)}(\tau_0 s^4 + s^3),$$

$$C = -2\xi^2 + \frac{1}{a_1}(a_5 - a_1a_6) - \frac{s^2}{a_1}(a_4 + a_1a_7),$$

$$D = \xi^4 - \frac{\xi^2}{a_1}(a_5 - a_1a_6) + \frac{s^2\xi^2}{a_1}\{a_4 + a_1a_7\} + \frac{s^4}{a_1}a_4a_7 + \frac{s^2}{a_1}a_4a_6,$$

and

$$a_1 = \frac{\mu + K}{\lambda + \mu + \mu_0 H_0^2}, \quad a_2 = \frac{K}{\lambda + \mu + \mu_0 H_0^2}, \quad a_3 = \frac{\rho\, c_1^2}{\lambda + \mu + \mu_0 H_0^2},$$

$$a_4 = \frac{\rho + \varepsilon_0\mu_0^2 H_0^2}{\lambda + \mu + \mu_0 H_0^2}c_1^2, \quad a_5 = \frac{K c_1^2}{\gamma\bar{\omega}^2}, \quad a_6 = 2\frac{K c_1^2}{\gamma\bar{\omega}^2}, \quad a_7 = \frac{\rho\, j}{\gamma}c_1^2.$$

The solutions of Eqs. 21–23 satisfying the radiation conditions that $\tilde{\psi}_1$, $\tilde{\psi}_2$, $\tilde{h}_0$, $\tilde{T}$, and $\tilde{\phi}_3$ tend to zero as y tends to infinity can be written as

$$\tilde{\psi}_1 = A_1 e^{-\lambda_1 y} + A_2 e^{-\lambda_2 y}, \tag{24}$$

$$\tilde{\psi}_2 = B_1 \mathrm{e}^{-\lambda_3 y} + B_2 \mathrm{e}^{-\lambda_4 y}, \tag{25}$$

$$\tilde{h}_0 = C \mathrm{e}^{-\lambda_5 y}, \tag{26}$$

$$\tilde{T} = m_1 A_1 \mathrm{e}^{-\lambda_1 y} + m_2 A_2 \mathrm{e}^{-\lambda_2 y}, \tag{27}$$

$$\tilde{\phi}_3 = m_3 B_1 \mathrm{e}^{-\lambda_3 y} + m_4 B_2 \mathrm{e}^{-\lambda_4 y}, \tag{28}$$

where

$$\lambda_1^2, \lambda_2^2 = \frac{1}{2}\left(A \pm \sqrt{A^2 - 4B}\right), \quad \lambda_3^2, \lambda_4^2 = \frac{1}{2}\left(C \pm \sqrt{C^2 - 4D}\right), \quad \lambda_5^2 = \xi^2 + \frac{c_1^2}{c^2} s^2,$$
$$m_1 = \frac{\lambda_1^2 - E}{F}, \quad m_2 = \frac{\lambda_2^2 - E}{F}, \quad m_3 = \frac{\lambda_3^2 - G}{H}, \quad m_4 = \frac{\lambda_4^2 - G}{H},$$

and

$$E = \xi^2 + \frac{a_4}{(1 + a_1)} s^2, \quad F = \frac{a_3}{(1 + a_1)}(1 + \tau_1 s),$$
$$G = \xi^2 + \frac{a_4}{a_1} s^2, \quad H = -\frac{a_2}{a_1}.$$

4 Boundary Conditions

4.1 Mechanical Boundary Conditions

The boundary surface is subjected to a normal force

(i)
$$\sigma_{22} + T_{22} - T_{22}^0 = -P_1 f_1(x, t), \tag{29}$$

(ii)
$$\sigma_{21} = 0, \tag{30}$$

(iii)
$$m_{23} = 0, \tag{31}$$

where P_1 is the magnitude of the force, $f_1(x, t)$ is the known function, and T_{22}, T_{22}^0 are components of the Maxwell stress tensor in a magneto-micropolar thermoelastic medium and vacuum, respectively.

4.2 Thermal Boundary Conditions

(iv) The temperature at the boundary surface $y = 0$ is expressed as

$$T = P_2 f_2(x, t), \tag{32}$$

where P_2 is the constant temperature applied on the boundary and $f_2(x, t)$ is the known function.

(v) The transverse components of the magnetic field intensity are continuous across the boundary surface $y = 0$;

$$h(x, 0, t) = h^0(x, 0, t). \tag{33}$$

(vi) The transverse components of the electric field intensity are continuous across the boundary surface $y = 0$;

$$E_1(x, 0, t) = E_1^0(x, 0, t). \tag{34}$$

Since the relative permeabilities are very nearly unity, it follows from Eqs. 5, 16, and 33 that $T_{22} = T_{22}^0$ and the condition in Eq. 29 reduces to

$$\sigma_{21} = -P_1 f_1(x, t). \tag{35}$$

Applying the Laplace and Fourier transforms defined by Eq. 20 on boundary conditions in Eqs. 29–35 and with the help of Eqs. 3, 5, 9, 10, 16–18 and considering $P_1' = \frac{P_1}{\nu T_0}$, $P_2' = \frac{P_2}{T_0}$ (after suppressing the dashes), we obtain the components of normal strain, stresses, temperature distribution, and induced magnetic field (in vacuum) as

$$\tilde{e}_{22} = \frac{1}{\Delta}\left[\lambda_1^2\Delta_1 \mathrm{e}^{-\lambda_1 y} + \lambda_2^2\Delta_2 \mathrm{e}^{-\lambda_2 y} - i\xi\left(\lambda_3\Delta_3 \mathrm{e}^{-\lambda_3 y} + \lambda_4\Delta_4 \mathrm{e}^{-\lambda_4 y}\right)\right], \tag{36}$$

$$\begin{aligned}\tilde{\sigma}_{22} = \frac{1}{\Delta}\Big[&\left(\lambda_1^2 - \xi^2 a_8 - \tau m_1\right)\Delta_1 \mathrm{e}^{-\lambda_1 y} + \left(\lambda_2^2 - \xi^2 a_8 - \tau m_2\right)\Delta_2 \mathrm{e}^{-\lambda_2 y} \\ &- (a_8 - 1)\, i\xi\left(\lambda_3\Delta_3 \mathrm{e}^{-\lambda_3 y} + \lambda_4\Delta_4 \mathrm{e}^{-\lambda_4 y}\right)\Big],\end{aligned} \tag{37}$$

$$\begin{aligned}\tilde{\sigma}_{21} = \frac{1}{\Delta}\Big[&i\xi\,(a_9 + a_{10})\left\{\lambda_1\Delta_1 \mathrm{e}^{-\lambda_1 y} + \lambda_2\Delta_2 \mathrm{e}^{-\lambda_2 y}\right\} \\ &+ \left(\xi^2 a_9 + \lambda_3^2 a_{10} + m_3 a_{11}\right)\Delta_3 \mathrm{e}^{-\lambda_3 y} \\ &+ \left(\xi^2 a_9 + \lambda_4^2 a_{10} + m_4 a_{11}\right)\Delta_4 \mathrm{e}^{-\lambda_4 y}\Big],\end{aligned} \tag{38}$$

$$\tilde{m}_{23} = \frac{1}{\Delta}\left[-\lambda_3 m_3\Delta_3 \mathrm{e}^{-\lambda_3 y} - \lambda_4 m_4\Delta_4 \mathrm{e}^{-\lambda_4 y}\right], \tag{39}$$

$$\tilde{T} = \frac{1}{\Delta}\left[m_1\Delta_1 \mathrm{e}^{-\lambda_1 y} + m_2\Delta_2 \mathrm{e}^{-\lambda_2 y}\right], \tag{40}$$

$$\tilde{h}^0 = \frac{1}{\Delta}\Delta_5 \mathrm{e}^{-\lambda_5 y}, \tag{41}$$

where

$$\begin{aligned}\Delta = a_{12}\lambda_5(m_3\lambda_3 - m_4\lambda_4)\Big[&\left\{\xi^2 + (a_9 + a_{10}) + a_{11}m_4\right\}\left\{(\lambda_1^2 m_2 - \lambda_2^2 m_1)\right. \\ &\left.+\xi^2 a_8(m_1 - m_2)\right\} - \xi^2\lambda_4(a_8 - 1)(a_9 + a_{10}) \\ &\times(\lambda_2 m_1 - \lambda_1 m_2)\Big] - a_{12}\lambda_5 m_4\lambda_4\left[a_{11}(m_3 - m_4)\right.\end{aligned}$$

$$\times \left\{(\lambda_1^2 m_2 - \lambda_2^2 m_1) + \xi^2 a_8 (m_1 - m_2)\right\}$$
$$-\xi^2 (a_8 - 1)(\lambda_3 - \lambda_4)(a_9 + a_{10})(\lambda_2 m_1 - \lambda_1 m_2)\Big],$$

$$\Delta_1 = a_{12}\lambda_5 \Big[\left\{P_1 \tilde{f}_1(\xi, s) m_2 + P_2 \tilde{f}_2(\xi, s)(\lambda_2^2 - \xi^2 a_8 - \tau m_2)\right\}$$
$$\times \left\{\xi^2 (a_9 + a_{10})(m_4\lambda_4 - m_3\lambda_3) + a_{11} m_3 m_4 (\lambda_4 - \lambda_3)\right\}$$
$$-P_2 \tilde{f}_2(\xi, s)\xi^2 (a_9 + a_{10})(a_8 - 1)\lambda_2\lambda_3\lambda_4 (m_3 - m_4)\Big],$$

$$\Delta_2 = -a_{12}\lambda_5 \Big[\left\{P_1 \tilde{f}_1(\xi, s) m_1 + P_2 \tilde{f}_2(\xi, s)(\lambda_1^2 - \xi^2 a_8 - \tau m_1)\right\}$$
$$\times \left\{\xi^2 (a_9 + a_{10})(m_4\lambda_4 - m_3\lambda_3) + a_{11} m_3 m_4 (\lambda_4 - \lambda_3)\right\}$$
$$-P_2 \tilde{f}_2(\xi, s)\xi^2 (a_9 + a_{10})(a_8 - 1)\lambda_1\lambda_3\lambda_4 (m_3 - m_4)\Big],$$

$$\Delta_3 = a_{12}\lambda_5 i\xi m_4\lambda_4 (a_9 + a_{10}) \Big[P_1 \tilde{f}_1(\xi, s)(\lambda_2 m_1 - \lambda_1 m_2) + P_2 \tilde{f}_2(\xi, s)$$
$$\times \left\{(\lambda_1^2 - \xi^2 a_8 - \tau m_1)\lambda_2 \right.$$
$$\left. - (\lambda_2^2 - \xi^2 a_8 - \tau m_2)\lambda_1\right\}\Big],$$

$$\Delta_4 = -a_{12}\lambda_5 i\xi m_3\lambda_3 (a_9 + a_{10}) \Big[P_1 \tilde{f}_1(\xi, s)(\lambda_2 m_1 - \lambda_1 m_2) + P_2 \tilde{f}_2(\xi, s)$$
$$\times \left\{(\lambda_1^2 - \xi^2 a_8 - \tau m_1)\lambda_2 \right.$$
$$\left. - (\lambda_2^2 - \xi^2 a_8 - \tau m_2)\lambda_1\right\}\Big],$$

$$\Delta_5 = -a_{11} s^2 m_3 m_4 (\lambda_3 - \lambda_4) \Big[P_1 \tilde{f}_1(\xi, s)(\lambda_2 m_1 - \lambda_1 m_2) + P_2 \tilde{f}_2(\xi, s)$$
$$\times \left\{(\lambda_1^2 - \xi^2 a_8 - \tau m_1)\lambda_2 \right.$$
$$\left. - (\lambda_2^2 - \xi^2 a_8 - \tau m_2)\lambda_1\right\}\Big],$$

and

$$\tau = 1 + \tau_1 s, \quad a_8 = \frac{\lambda}{\lambda + 2\mu + K}, \quad a_9 = \frac{\mu}{\lambda + 2\mu + K},$$
$$a_{10} = \frac{\mu + K}{\lambda + 2\mu + K}, \quad a_{11} = \frac{K}{\lambda + 2\mu + K}, \quad a_{12} = \frac{\rho c^2}{\nu T_0}.$$

5 Applications

We take $f_1(x, t)$ and $f_2(x, t)$ as

$$(f_1(x, t),\, f_2(x, t)) = \begin{cases} (g_1(x),\, g_2(x))\delta(t) & \text{for concentrated source,} \\ (g_1(x),\, g_2(x))H(t) & \text{for continuous source} \end{cases} \tag{42}$$

where $\delta(t)$ is the Dirac delta function and $H(t)$ is the Heaviside distribution function. $g_1(x)$ and $g_2(x)$ are known functions.

5.1 Uniformly Distributed Source (Concentrated or Continuous)

In this case,

$$(g_1(x), g_2(x)) = \begin{cases} 1 & \text{if } |x| \leq \text{a}, \\ 0 & \text{if } |x| > \text{a} \end{cases} \tag{43}$$

where a is the dimensionless strip width. With the help of Eqs. 18 and 20, the Laplace and Fourier transforms of Eqs. 42 and 43 are given by (where Laplace and Fourier transforms of $\delta(t)$ and $H(t)$ are 1 and $1/s$, respectively)

$$(\tilde{f}_1(\xi, s), \tilde{f}_2(\xi, s)) = \begin{cases} (2\sin(\xi\, a)/\xi), \quad \xi \neq 0 & \text{for concentrated source,} \\ (2\sin(\xi\, a)/\xi) \cdot 1/s, \quad \xi \neq 0 & \text{for continuous source} \end{cases} \tag{44}$$

5.2 Linearly Distributed Source (Concentrated or Continuous)

In this case,

$$(g_1(x), g_2(x)) = \begin{cases} 1 - \frac{|x|}{a} & \text{if } |x| \leq \text{a}, \\ 0 & \text{if } |x| > \text{a} \end{cases} \tag{45}$$

With the help of Eqs. 18 and 20, the Laplace and Fourier transforms of Eqs. 42 and 45 are given by

$$(\tilde{f}_1(\xi, s), \tilde{f}_2(\xi, s)) = \begin{cases} 2[1 - \cos(\xi\, a)]/\xi^2 a, & \text{for concentrated source,} \\ 2[1 - \cos(\xi\, a)]/s\xi^2 a, & \text{for continuous source} \end{cases} \tag{46}$$

The corresponding solutions are obtained for a uniformly and linearly (concentrated or continuous) distributed source by substituting the values of $\tilde{f}_1(\xi, s)$ and $\tilde{f}_2(\xi, s)$ from Eqs. 44 and 46 in Eqs. 36–41.

5.3 Particular Case

If $H_0 \to 0$ in Eqs. 36–41, we obtain the components of displacements and stresses in a micropolar thermoelastic medium with the following changed values of a_1, a_2, a_3, and a_4 as

$$a_1 = \frac{\mu + K}{\lambda + \mu}, \quad a_2 = \frac{K}{\lambda + \mu}, \quad a_3 = a_4 = \frac{\lambda + 2\mu + K}{\lambda + \mu}.$$

6 Inversion of the Transforms

To obtain the solution of the problem in the physical domain, we must invert the transforms in Eqs. 24–28 and 36–41, for the L–S and G–L theories of thermoelasticity. These expressions are functions of y, the parameters of Laplace and Fourier transforms s and ξ, respectively, and hence are of the form $\tilde{f}(\xi, y, s)$. To get the function $\bar{f}(x, y, s)$ in the physical domain, first we invert the Fourier transform using

$$\bar{f}(x, y, s) = \frac{1}{2\pi} \int_{-\infty}^{\infty} \mathrm{e}^{-i\xi x} \tilde{f}(\xi, y, s) \mathrm{d}\xi = \frac{1}{\pi} \int_{0}^{\infty} (\cos(\xi x) f_e - i \sin(\xi x) f_0) \, \mathrm{d}\xi, \tag{47}$$

where f_e and f_0 are, respectively, even and odd parts of the function $\tilde{f}(\xi, y, s)$. Thus, Eq. 47 gives us the Laplace transform $\bar{f}(x, y, s)$ of the function $f(x, y, t)$.

Then, for the fixed values of ξ, x, and y, $\bar{f}(x, y, s)$in Eq. 47 can be considered as the Laplace transform $\bar{g}(s)$ of $g(t)$. Following Honig and Hirdes [21], the Laplace transformed function $\bar{g}(s)$ can be inverted as given below. The function $g(t)$ can be obtained by using

$$g(t) = \frac{1}{2\pi i} \int_{X-i\infty}^{X+i\infty} \mathrm{e}^{st} \bar{g}(s) \, \mathrm{d}s, \tag{48}$$

where X is an arbitrary real number greater than all the real parts of the singularities of $\bar{g}(s)$. Taking $s = X + iz$, we get

$$g(t) = \frac{\mathrm{e}^{Xt}}{2\pi i} \int_{-\infty}^{\infty} \mathrm{e}^{i t z} \bar{g}(X + iz) \, \mathrm{d}z. \tag{49}$$

Now, taking $\mathrm{e}^{-Xt} g(t)$ as $h(t)$ and expanding it as a Fourier series in $[0, 2L]$, we obtain approximately the formula,

$$g(t) = g_\infty(t) + E_\mathrm{D},$$

where

$$g_\infty(t) = \frac{X_0}{2} + \sum_{k=1}^{\infty} X_k, \quad 0 \le t \le 2L,$$

and

$$X_k = \left(\frac{\mathrm{e}^{Xt}}{L}\right) \mathrm{Re}\left[\mathrm{e}^{\frac{ik\pi t}{L}} \bar{g}\left(X + \left(\frac{ik\pi}{L}\right)\right)\right]. \tag{50}$$

E_D is the discretization error and can be made arbitrarily small by choosing X sufficiently large. The values of X and L are chosen according to the criteria outlined by Honig and Hirdes [21].

Since the infinite series in Eq. 50 can be summed up only to a finite number of N terms, the approximate value of $g(t)$ becomes

$$g_N(t) = \frac{X_0}{2} + \sum_{k=1}^{N} X_k, \quad 0 \le t \le 2L. \tag{51}$$

Now, we introduce a truncation error E_T, that must be added to the discretization error to produce the total approximate error in evaluating $g(t)$ using the above formula. To accelerate the convergence, the discretization error and then the truncation error are reduced by using the 'Korrecktur method' and the 'ε-algorithm,' respectively, as given by Honig and Hirdes [21].

The Korrecktur method formula, to evaluate the function $g(t)$, is

$$g(t) = g_\infty(t) - \mathrm{e}^{-2XL} g_\infty(2L + t) + E'_D,$$

where

$$\left|E'_D\right| \ll |E_D|\,.$$

Thus, the approximate value of $g(t)$ becomes

$$g_{N_k}(t) = g_N(t) - \mathrm{e}^{-2XL} g_{N'}(2L + t), \tag{52}$$

where N' is an integer such that $N' < N$.

We shall now describe the ε-algorithm, which is used to accelerate the convergence of the series in Eq. 51. Let N be an odd natural number and $S_m = \sum_{k=1}^{m} X_k$ be the sequence of partial sums of Eq. 51. We define the 'ε-sequence' by

$$\varepsilon_{0,m} = 0, \quad \varepsilon_{1,m} = S_m, \quad \varepsilon_{n+1,m} = \varepsilon_{n-1,m+1} + \frac{1}{\varepsilon_{n,m+1} - \varepsilon_{n,m}}, \quad n, m = 1, 2, 3\ldots$$

The sequence $\varepsilon_{1,1}, \varepsilon_{3,1}, \ldots, \varepsilon_{N,1}$ converges to $g(t) + E_D - \frac{X_0}{2}$ faster than the sequence of partial sums S_m, $m = 1, 2, 3\ldots$. The actual procedure to invert the Laplace transform consists of Eq. 52 together with the 'ε-algorithm'.

The last step is to calculate the integral in Eq. 47. The method for evaluating this integral is described in Press et al. [22], which involves the use of Romberg's integration with an adaptive step size. This also uses the results from successive refinements of the extended trapezoidal rule followed by extrapolation of the results to the limit when the step size tends to zero.

7 Numerical Results and Discussion

The analysis is conducted for a magnesium crystal-like material. Following Ref. [23], the values of the physical constants are

$$\lambda = 9.4 \times 10^{10}\,\mathrm{N \cdot m^{-2}}, \quad \mu = 4.0 \times 10^{10}\,\mathrm{N \cdot m^{-2}}, \quad K = 1.0 \times 10^{10}\,\mathrm{N \cdot m^{-2}},$$
$$\rho = 1.74 \times 10^{3}\,\mathrm{kg \cdot m^{-3}}, \quad \gamma = 0.779 \times 10^{-9}\,\mathrm{N}, \quad j = 0.2 \times 10^{-19}\,\mathrm{m^2}.$$

The thermal parameters are given by

$$c^* = 1.04 \times 10^{3}\,\mathrm{J \cdot kg^{-1} \cdot K^{-1}}, \quad K^* = 1.7 \times 10^{2}\,\mathrm{J \cdot m^{-1} \cdot s^{-1} \cdot K^{-1}},$$
$$\nu = 2.68 \times 10^{6}\,\mathrm{N \cdot m^{-2} \cdot K^{-1}}, \quad T_0 = 296\,K, \quad , \tau_0 = 0.02, \quad \tau_1 = 0.05$$

In numerical calculations, we considered the magnetic interference wave speed

$$a_0 = \sqrt{\frac{\mu_0 H_0^2}{\rho}} = 10^{3}\,\mathrm{m \cdot s^{-1}},$$

and

$$c = 3 \times 10^{8}\,\mathrm{m \cdot s^{-1}}, \quad \mu_0 = 4\pi \times 10^{-7}\,\mathrm{H \cdot m^{-1}}, \quad \varepsilon_0 = 1/36\pi \times 10^{-9}\,\mathrm{F \cdot m^{-1}}.$$

The computations are carried out for the dimensionless time $t = 0.5$ and dimensionless strip width $a = 0.3$, in the range $0 \le x \le 10$. The distribution of the dimensionless normal strain e_{22}, the dimensionless normal stress, σ_{22}, the dimensionless tangential couple stress m_{23}, and the dimensionless temperature distribution T with the dimensionless distance 'x' have been shown in Figs. 1, 2, 3, 4, 5, 6, 7, 8, 9, 10, 11, 12, 13, 14, 15, 16. The solid line and dashed line, for a magneto-micropolar thermoelastic medium, are represented as MMT1 (for L–S theory) and MMT2 (for G–L theory), respectively. The solid line with circles and dashed line with triangles, for micropolar thermoelastic medium are, represented as MT1 (for L–S theory) and MT2 (for G–L theory), respectively.

7.1 Uniformly Distributed Source

The variations of the normal strain e_{22}, normal stress σ_{22}, tangential couple stress m_{23}, and temperature distribution T with distance 'x' for MMT1, MMT2, MT1, and MT2, when a concentrated source is applied are shown in Figs. 1, 2, 3, and 4, respectively, and when a continuous source is applied are shown in Figs. 5, 6, 7, and 8, respectively.

7.1.1 Concentrated Source

Figure 1 depicts the variation of the normal strain e_{22}, and it is noted that its value is larger in the initial range $0 \le x \le 1$, for MMT1 as compared to the value for MMT2;

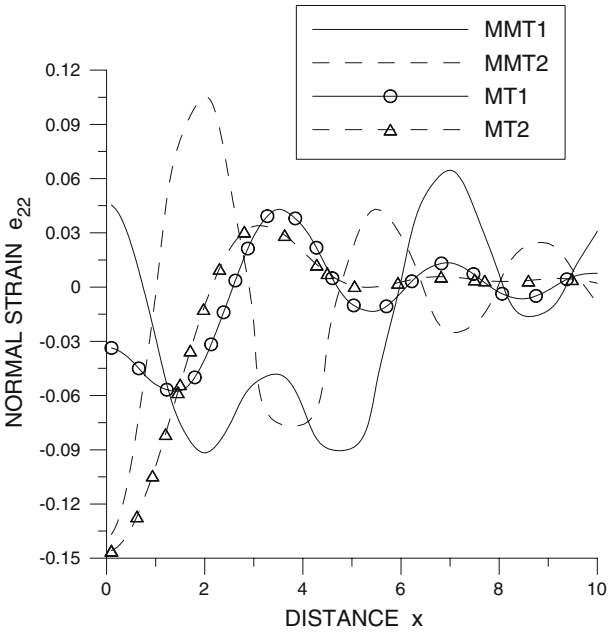

Fig. 1 Variation of normal strain e_{22} for magneto-micropolar thermoelastic medium, represented as MMT1 (for L–S theory) and MMT2 (for G–L theory), and for micropolar thermoelastic medium, represented as MT1 (for L–S theory) and MT2 (for G–L theory), with distance x

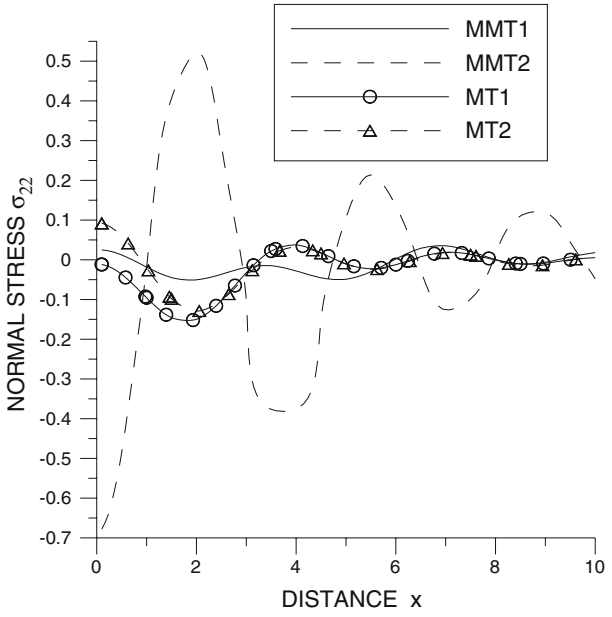

Fig. 2 Variation of normal stress σ_{22} with distance x; symbols same as in Fig. 1

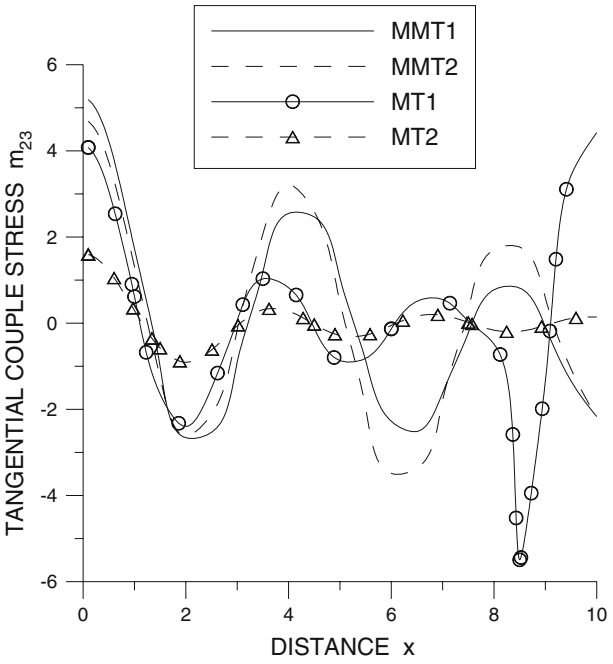

Fig. 3 Variation of tangential couple stress m_{23} with distance x; symbols same as in Fig. 1

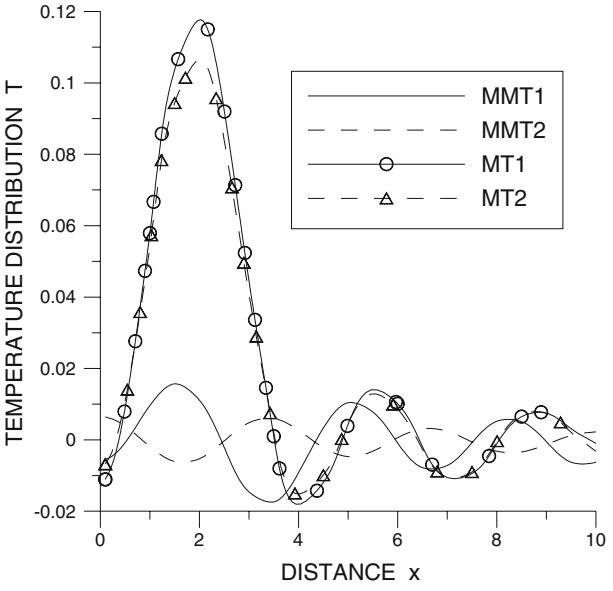

Fig. 4 Variation of temperature distribution T with distance x; symbols same as in Fig. 1

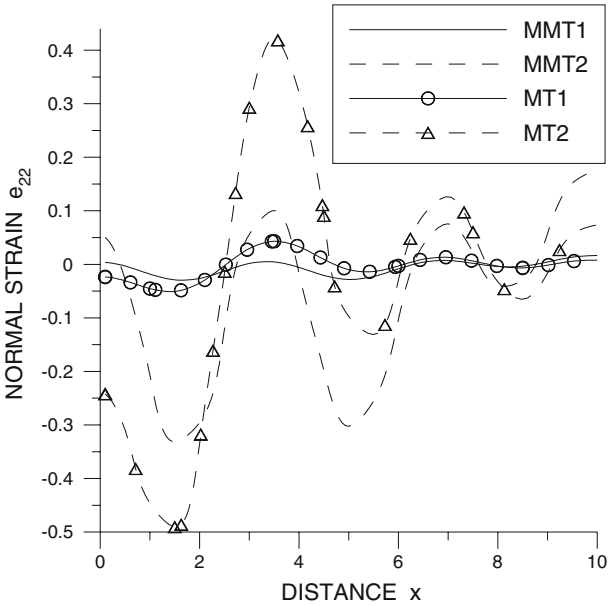

Fig. 5 Variation of normal strain e_{22} with distance x; symbols same as in Fig. 1

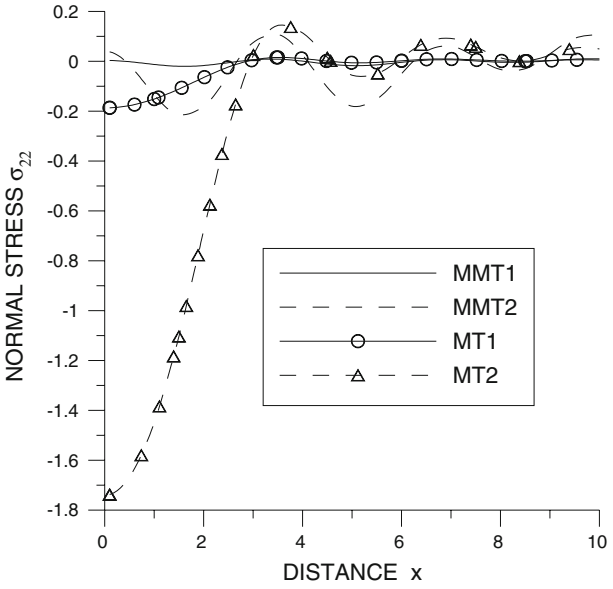

Fig. 6 Variation of normal stress σ_{22} with distance x; symbols same as in Fig. 1

and the behavior is reversed as x increases further in the range $1 \leq x \leq 3$. Very near to the point of application of the source, the value of the normal strain e_{22} is large for MT1 as compared to the value for MT2; and as x increases further, the variation of

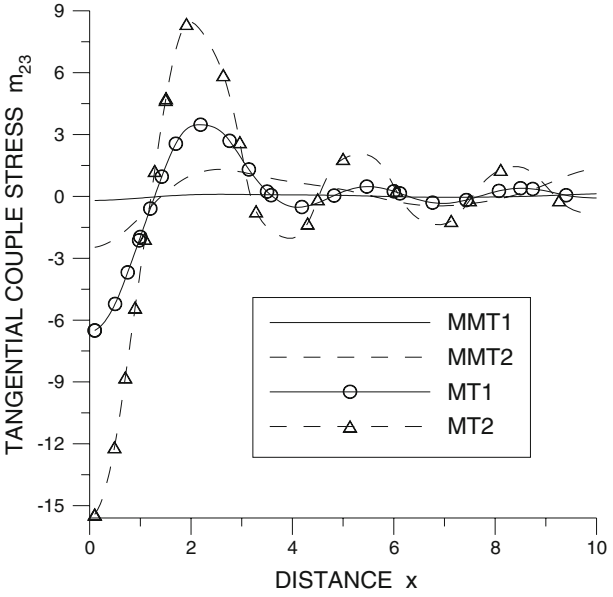

Fig. 7 Variation of tangential couple stress m_{23} with distance x; symbols same as in Fig. 1

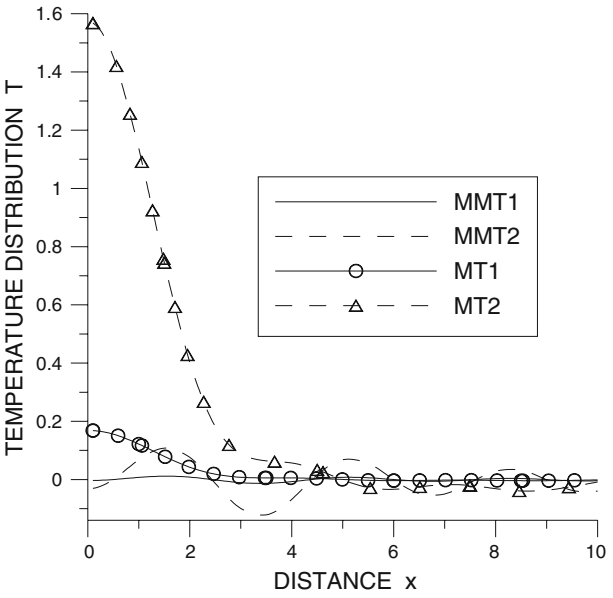

Fig. 8 Variation of temperature distribution T with distance x; symbols same as in Fig. 1

the normal strain e_{22} is oscillatory for MT1 and MT2. The value of the normal strain e_{22} for MMT2 has been shown in Fig. 1 by multiplying its original value by 10^{-1}. It is observed from Fig. 2 that very near to the point of application of the source, due

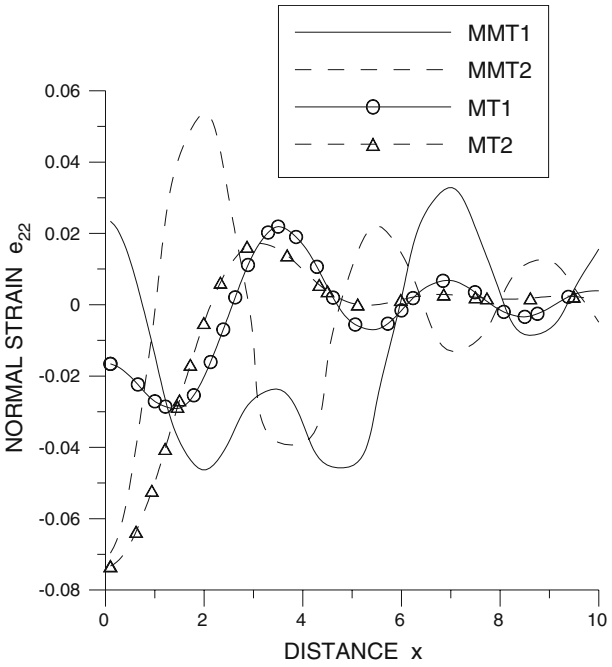

Fig. 9 Variation of normal strain e_{22} with distance x; symbols same as in Fig. 1

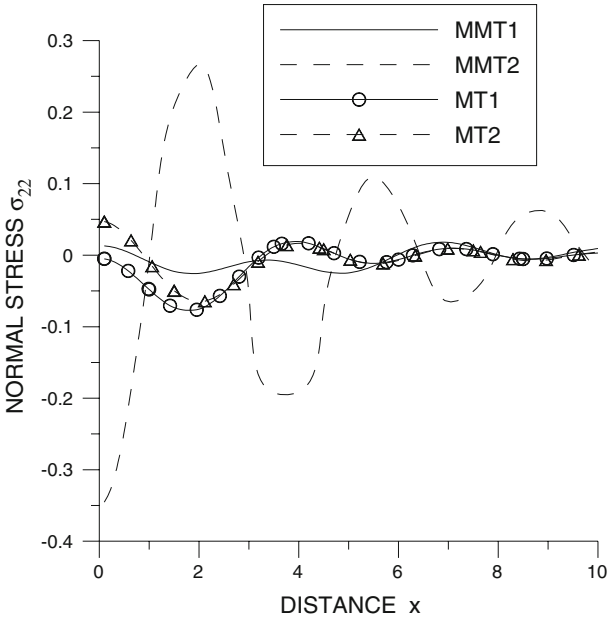

Fig. 10 Variation of normal stress σ_{22} with distance x; symbols same as in Fig. 1

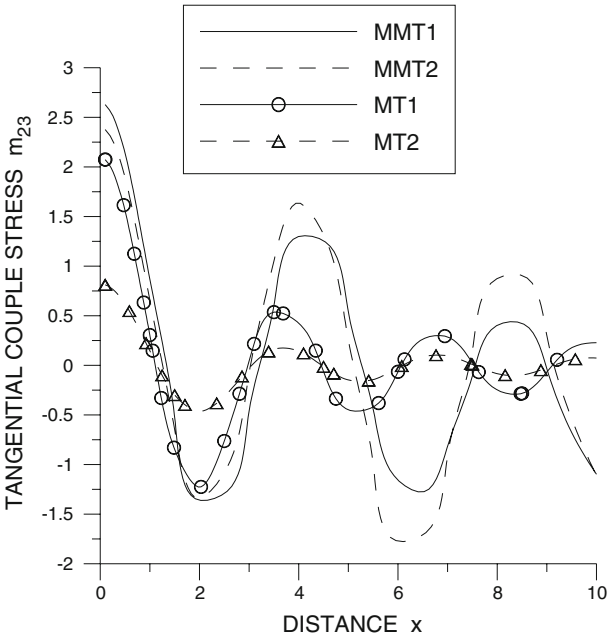

Fig. 11 Variation of tangential couple stress m_{23} with distance x; symbols same as in Fig. 1

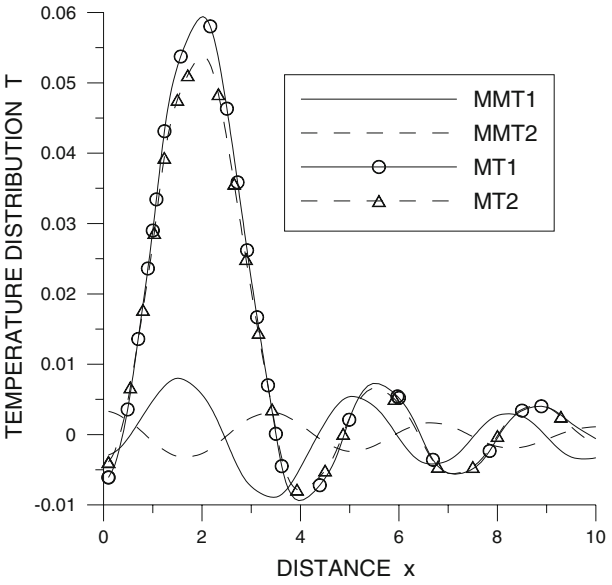

Fig. 12 Variation of temperature distribution T with distance x; symbols same as in Fig. 1

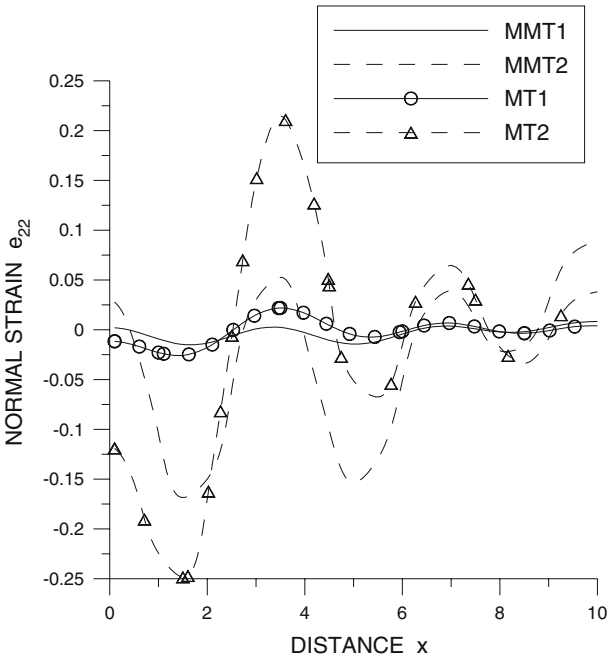

Fig. 13 Variation of normal strain e_{22} with distance x; symbols same as in Fig. 1

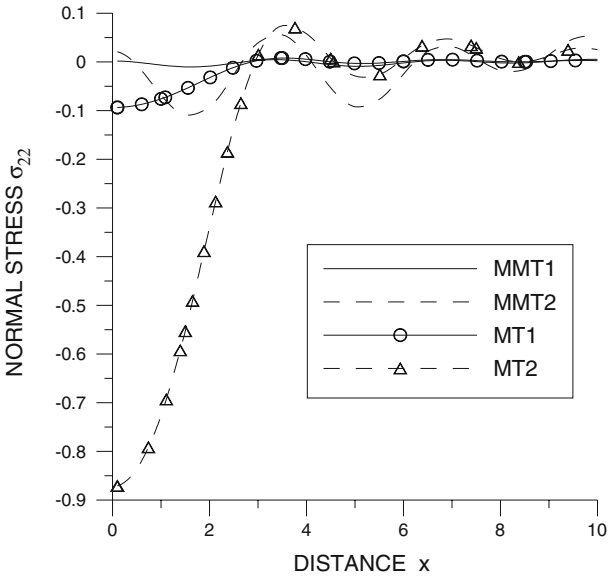

Fig. 14 Variation of normal stress σ_{22} with distance x; symbols same as in Fig. 1

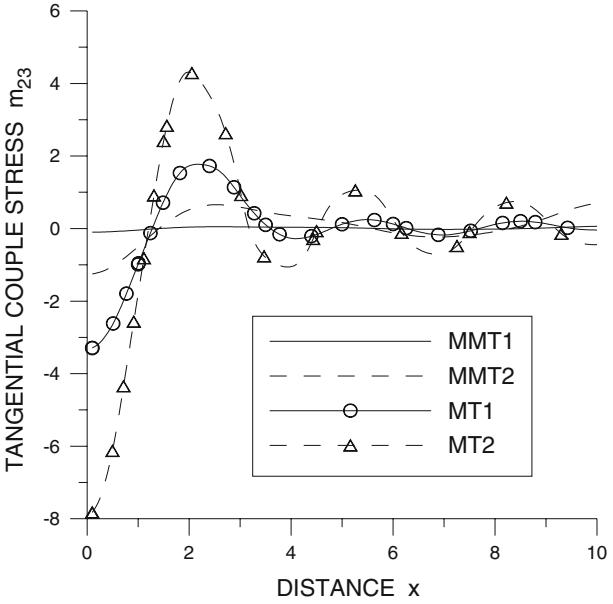

Fig. 15 Variation of tangential couple stress m_{23} with distance x; symbols same as in Fig. 1

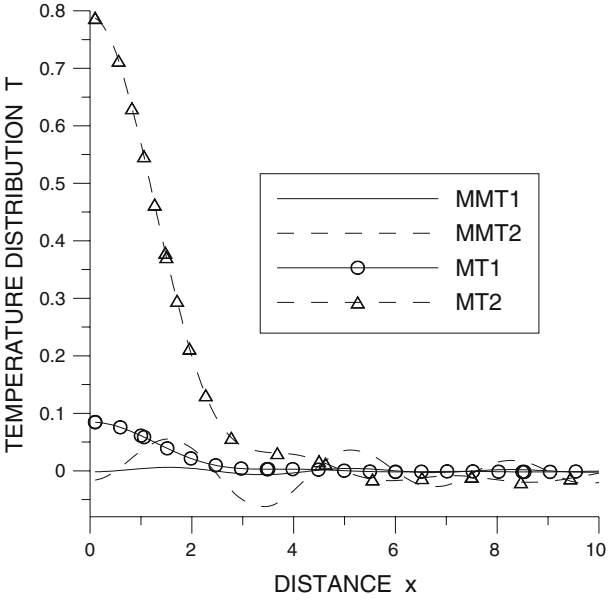

Fig. 16 Variation of temperature distribution T with distance x; symbols same as in Fig. 1

to the magnetic effect, the value of the normal stress σ_{22} is very small for MMT2 as compared to the value for MT2, but its value is slightly larger for MMT1 as compared to the value for MT1, and as x increases further, the variation is oscillatory in nature.

Figure 3 depicts that initially, the value of the tangential couple stress m_{23} is larger with the magnetic effect for MMT1 and MMT2 as compared to that without the magnetic effect for MT1 and MT2. As 'x' increases further, it shows an oscillatory behavior. The values of the tangential couple stress m_{23} are shown in Fig. 3, the original values of which have been downscaled through multiplication by 10^{-1} and 10^{-3} for the cases of MT1 and MT2, respectively. It is observed from Fig. 4 that, very near to the application of the source, the value of the temperature distribution T is larger for MMT2 as compared to the value for MMT1 and then starts oscillating with an increase in distance x. The variation of the temperature distribution T for MT1 and MT2 is similar over the whole range, except the peak value of the temperature distribution is larger for MT1 as compared to MT2 in the range $1 \leq x \leq 3$.

7.1.2 Continuous Source

Figure 5 depicts that in the initial range $0 \leq x \leq 2$, the values of the normal strain e_{22} are large for MMT2 and slightly large for MMT1 as compared to the values for MT2 and MT1, respectively, and as 'x' increases further, the variation is oscillatory. The values of the normal strain e_{22} for MMT2 and MT2 are shown in Fig. 5 by multiplying the original values by 10. From Fig. 6 we observe that, due to the magnetic effect, the values of the normal stress σ_{22} are large for MMT1 and MMT2 in comparison with MT1 and MT2, respectively, and the value for MT2 is very small as compared to the value for MT1 initially in the range $0 \leq x \leq 2$, and then starts oscillating with an increase in distance x. The values of the normal stress σ_{22} for MMT2 and MT2 are shown in Fig. 6 by multiplying the original values by 10.

The variation of the tangential couple stress m_{23}, depicted in Fig. 7, shows that initially in the range $0 \leq x \leq 1$, due to the magnetic effect, the value of the tangential couple stress m_{23} is very small for MT2 in comparison to the value for MMT2, but in this range, the value is slightly larger for MMT1 in comparison to the value for MT1. In the range $1 \leq x \leq 3$, the peak value is larger for MT2 in comparison to the value for MT1. As 'x' increases further, the behavior is oscillatory. The value of the tangential couple stress m_{23} for MMT2 is shown in Fig. 7 by multiplying its original value by 10. Figure 8 depicts that due to the magnetic effect, the values of the temperature distribution T are small for MMT1 and MMT2 in comparison with MT1 and MT2, respectively, and the value for MT2 is very large as compared to the value for MT1 initially in the range $0 \leq x \leq 2$, and then starts oscillating with an increase in distance x. The values of the temperature distribution T for MMT2 and MT2 are shown in Fig. 8 by multiplying the original values by 10.

7.2 Linearly Distributed Source

The variations of the normal strain e_{22}, normal stress σ_{22}, tangential couple stress m_{23}, and temperature distribution T with distance 'x' for MMT1, MMT2, MT1, and MT2, when a concentrated source is applied, are shown in Figs. 9, 10, 11, and 12, respectively, and when a continuous source is applied, are shown in Figs. 13, 14, 15, and 16, respectively.

7.2.1 Concentrated Source

Figures 9, 10, 11, and 12 depict that the variations of the normal strain e_{22}, normal stress σ_{22}, tangential couple stress m_{23}, and temperature distribution T are of a similar nature as in the case of a uniformly distributed source, with a difference in their magnitude. From Fig. 11, we observe that the variation of the tangential couple stress m_{23} for MT1 is changed in the range $8 \leq x \leq 10$.

7.2.2 Continuous Source

Figures 13, 14, 15, and 16 depict that the variation of the normal strain e_{22}, normal stress σ_{22}, tangential couple stress m_{23}, and temperature distribution T are of similar nature as in the case of a uniformly distributed source, with a difference in their magnitude.

8 Conclusion

The Laplace and Fourier transform techniques are used to derive the components of normal strain, normal stress, tangential couple stress, and temperature distribution.

The behaviors of variations of normal strain, normal stress, tangential couple stress, and temperature distribution for both theories of generalized thermoelasticity, for a uniformly distributed source (concentrated or continuous) and a linearly distributed source (concentrated or continuous), are of similar nature with a difference in their magnitude.

Acknowledgment One of the authors Mr. Rupender is thankful to the University Grants Commission for the financial support.

References

1. L. Knopoff, J. Geophys. Res. **60**, 441 (1955)
2. A. Banos, Phys. Rev. **104**, 300 (1956)
3. P. Chadwick, IX Congress. Inter. de Mecan. Appl. **7**, 143 (1957)
4. C.M. Purushothama, Proc. Camb. Philol. Soc. **62**, 541 (1966)
5. A.J. Willson, Proc. Camb. Philol. Soc. **62**, 91 (1966)
6. A.C. Eringen, J. Math. Mech. **15**, 909 (1966)
7. A.C. Eringen, J. Math. Mech. **16**, 1 (1966)
8. A.C. Eringen, in *Continuum Physics*, ed. by A.C. Eringen (Academic Press, New York, 1976), pp. 205–267
9. H. Lord, Y. Shulman, J. Mech. Phys. Solids **15**, 299 (1967)
10. I.M. Muller, Arch. Ration. Mech. Anal. **41**, 319 (1971)
11. A.E. Green, N. Laws, Arch. Ration. Mech. Anal. **45**, 47 (1972)
12. A.E. Green, K.A. Lindsay, J. Elasticity **2**, 1 (1972)
13. E.S. Suhubi, in *Continuum Physics*, ed. by A.C. Eringen (Academic Press, New York, 1975), Part 2, Chap. 2
14. S. Kaliski, Bull. Acad. Polit. Sci. Ser. Sci. Tech. **16**, 7 (1968)
15. S. Kaliski, W. Nowacki, Bull. Acad. Polit. Sci. Ser. Sci. Tech. **18**, 155 (1970)
16. W. Nowacki, Proc. Vib. Probl. **12**, 105 (1971)
17. D.S. Chandrasekharaiah, Tensor (N.S.) **25**, 287 (1972)

18. D.S. Chandrasekharaiah, J. Math. Phys. Sci. **9**, 1 (1975)
19. M.A. Ezzat, H.M. Youssef, Int. J. Eng. Sci. **42**, 6319 (2005)
20. A. Baksi, R.K. Bera, L. Debnath, Int. J. Eng. Sci. **43**, 1419 (2005)
21. G. Honig, U. Hirdes, J. Comput. Appl. Math. **10**,113 (1984)
22. W.H. Press, S.A. Teukolshy, W.T. Vellerling, B.P. Flannery, *Numerical Recipes in FORTRAN*, 2nd edn. (Cambridge University Press, Cambridge, 1986)
23. A.C. Eringen, Int. J. Eng. Sci. **22**, 1113 (1984)